

AN OVERVIEW OF ENSO SIGNATURE ON THE SURFACE PARAMETERS OF THE TROPICAL PACIFIC OCEAN

Thierry DELCROIX *

Abstract

The ENSO (El Niño Southern Oscillation) phenomenon is the planet's most powerful climatic event at the interannual time scale. In this note, the ENSO-related variability is described and analysed for key tropical Pacific oceanic and atmospheric parameters. These parameters consist of sea-surface temperature and salinity, 0/450 dbar dynamic height anomaly (*i. e.*, an alias for sea level), surface wind and precipitation collected during the 1961-1995 period. The ENSO-related signals are extracted from an Empirical Orthogonal Function (EOF) analysis performed on the low-pass filtered time series. For each parameter, the EOF analysis pinpoints the locations and times of notable ENSO-related variations in a concise manner.

Key words: *El Niño Southern Oscillation, Tropical Pacific, Climate.*

UN ESTUDIO DE LA FIRMA ENSO DE LOS PARÁMETROS SUPERFICIALES DEL OCEANO PACÍFICO TROPICAL

Resumen

El fenómeno ENSO (El Niño Oscilación del Sur) es el fenómeno climático más poderoso del planeta a una escala interanual. En esta nota, la variabilidad relacionada al ENSO, se describe y analiza para los parámetros claves oceánicos y atmosféricos del Pacífico tropical. Estos parámetros consisten en la temperatura superficial del mar y la salinidad, la anomalía de altura dinámica 0/450 dbar (esto es, un alias para el nivel del mar), viento superficial y la precipitación recolectada durante el período de 1961 a 1995. Se extraen las señales relacionadas al ENSO a partir del análisis de una Función Ortogonal Empírica (FOE) realizada en las series de tiempo filtradas de paso bajo. Para cada parámetro, el análisis FOE precisa las localizaciones y tiempos de las variaciones notables relacionadas al ENSO en una forma concisa.

Palabras claves: *El Niño Oscilación del Sur, Pacífico Tropical, clima.*

ÉTUDE DE LA SIGNATURE DE L'ENSO SUR LES PARAMÈTRES DE SURFACE DE L'OCÉAN PACIFIQUE TROPICAL

Résumé

À l'échelle interannuelle, le phénomène climatique El Niño Oscillation Australe (ENSO) constitue le signal climatique le plus puissant de la Planète. Cette note décrit et analyse la variabilité associée à ce phénomène dans le Pacifique tropical au cours de la période 1961-1995.

* SURTROPAC Group, IRD, BPA5, 98848 Noumea, New Caledonia; delcroix@noumea.ird.nc

L'accent est mis sur cinq paramètres considérés comme essentiels, à savoir: la température et la salinité de surface, l'anomalie de hauteur dynamique 0/450 dbar (un alias du niveau de la mer), le vent de surface et les précipitations. Le signal ENSO est décrit à partir d'une analyse en fonctions empiriques orthogonales des séries temporelles filtrées de manière à ne retenir que les variations de période supérieure à un an. Cette analyse précise de manière concise l'amplitude, la position géographique et la date d'apparition des anomalies associées à chaque paramètre.

Mot-clés : *El Niño Oscillation Australe, Pacifique Tropical, climat.*

INTRODUCTION

The tropical Pacific encompasses about half the circumference of the earth at the equator, and it is subject to dramatic climate variability on an interannual time scale: the El Niño Southern Oscillation (ENSO) phenomenon (see Philander, 1989). The goal of the present note is to provide an as-concise-as-possible analysis of some of the main features of the ENSO variability which is documented for sea-surface temperature (SST), sea-surface salinity (SSS), sea level through analysis of 0/450 dbar dynamic height anomalies, zonal and meridional surface wind stress together with precipitation (P). The relationships between the observed features of ENSO presented below and ENSO mechanisms are detailed in Delcroix (1998).

This note is organised as follows. A description of the 1961-1995 data used and processing procedures is given in section 1. A brief overview of the long-term means in SST, SSS, sea level, surface wind stress and precipitation follows in section 2, prior to analysing the ENSO variations in section 3. A conclusion is given in the last section.

1. THE DATA

The **sea-surface temperature** data were derived from the 1950-1994 monthly 2°-latitude by 2°-longitude gridded field of Reynolds and Smith (1994). The **sea-surface salinity** data (about 270,000 items) originate from a combination of bucket measurements collected via a ship-of-opportunity program, hydrocast and CTD measurements collected during more than two hundred research cruises, measurements taken by thermosalinographs installed on board merchant and research vessels, and thermosalinograph measurements from TAO moorings (see Donguy & Hénin, 1976; McPhaden *et al.*, 1990, Delcroix & Hénin, 1991; McPhaden, 1993; Hénin & Grelet, 1996; Delcroix *et al.*, 1996). Computation of the **surface dynamic height anomaly** was done from about 240,000 validated temperature profiles (mostly XBT measurements) collected in the tropical Pacific during 1979-1995. The temperature profile was converted into 0/450 dbar dynamic height anomaly using local mean T-S curves from Levitus *et al.* (1994). As noted by Rebert *et al.* (1985), the 0/450 dbar dynamic height anomaly is equivalent to sea level in the tropical Pacific. The **surface wind** was obtained from the monthly 2°-latitude by 2°-longitude FSU (Florida State University) pseudo wind-stress product (Goldenberg and O'Brien, 1981), in $\text{m}^2 \text{s}^{-2}$ units. The 1979-1995 **precipitation** data were taken from the analysis of Xie and Arkin (1996). Using all these

measurements, monthly 2°-latitude by 10°-longitude gridded fields were created for SST (1961-1994), SSS (1973-1995), sea level (1979-1995), zonal and meridional wind components (1961-1995), and P (1979-1995). Details are given in Delcroix (1998).

Climatological means and interannual variations were quantified for each parameter on the basis of the above mentioned fields. The climatological means were calculated over 1979-1992, a period common for each parameter. Time filtering was used to retain the interannual signals (*i. e.*, with period greater than 12 months) by filtering the monthly time series with a 25-month Hanning filter (Blackman & Tukey, 1958). The ENSO signal was then derived from an Empirical Orthogonal Function (EOF) analysis performed on the low frequency variations.

2. THE MEAN STRUCTURES

Maps of long-term mean SST, SSS, 0/450 dbar dynamic height anomaly (or sea level), pseudo-wind stress vector and precipitation are displayed in Figs. 1a-e. For SST we note the well-known decrease, poleward of about 15° latitude, and the westward increase in the equatorial band reflecting the presence of the equatorial upwelling in the east and of the warm pool in the west. For SSS, two high-salinity cores appear in the tropical Pacific, one in the vicinity of French Polynesia and the other north-west of the Hawaiian islands. Low-salinity waters are observed near the ITCZ (Inter Tropical Convergence Zone) and SPCZ (South Pacific Convergence Zone), as well as in the western equatorial Pacific. For the 0/450 dbar dynamic height anomaly, the main relief consists of: (a) the existence of a well-marked zonal slope with, for example, a 40 dyn cm difference between the eastern and western equatorial Pacific and, (b) almost zonally oriented ridges and troughs which mark the meridional boundaries of the mean surface geostrophic currents. For wind-stress vector, we found north-easterly winds in the northern hemisphere, and two systems of south-easterly winds separated by easterly winds in the southern hemisphere. This trade winds system converges to the ITCZ at about 5-10°N, and to the SPCZ which stretches from Papua New Guinea towards French Polynesia. For precipitation, the maximum values (> 2.5 m year⁻¹) are located in the ITCZ and SPCZ, these two zones being connected in the western Pacific warm pool. The minimum P values (< 0.5 m year⁻¹) appear in the NE and SE tropical Pacific. While representing different time periods and derived from different data and processing, these mean maps are in general agreement with previous studies dealing with long-term means (*e. g.*, Levitus, 1982; Reid, 1961; Wyrski & Meyers, 1976; Taylor, 1973).

3. THE ENSO-RELATED VARIATIONS

Bearing in mind the overview of the mean conditions, we now turn our attention to the ENSO-related variations derived from an EOF analysis performed on the low frequency variations. Only the EOF mode #1 are presented here (see Delcroix, 1998, for the other EOF modes), and the EOF time functions are compared to the 25-month filtered Southern Oscillation Index (SOI).

Sea-Surface Temperature. The interannual mode #1 EOF in SST (Fig. 2a) portrays coherent spatial variations in a large wedge-shaped area extending from the coast of the Americas to about 150°E at the equator. The largest changes are clearly

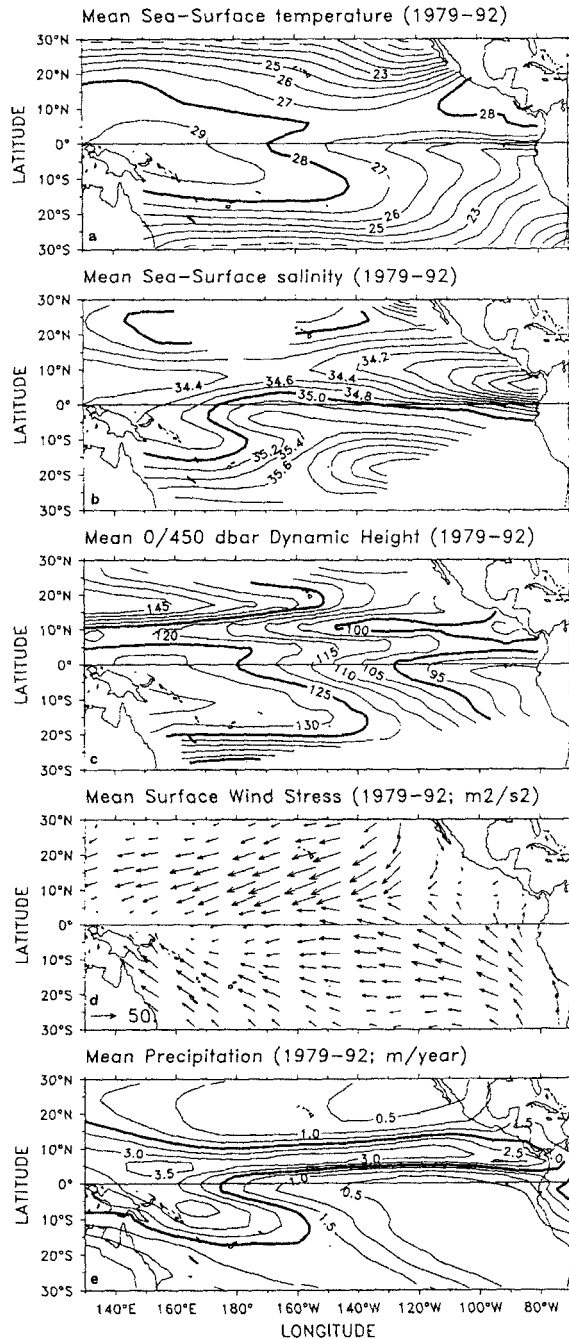


Fig. 1 - Long-term mean (a) sea-surface temperature, (b) sea-surface salinity, (c) 0/450 dbar dynamic height anomaly (d) surface wind stress and (e) precipitation. Units are (a) Celsius, (c) dyn cm, (d) 50 m²s⁻² for the eastward arrow drawn in Australia, and (e) m/year.

centred at or slightly south of the equator. There are opposite SST changes with small amplitude in a boomerang-shaped area stretching from the far western equatorial Pacific towards the extra tropical regions of each hemisphere. The EOF time function precisely shows the distinctive El Niño and La Niña periods: the correlation coefficient at zero lag with the filtered SOI is as high as 0.95. The product between the time function and spatial patterns results in warmer (colder) than average SST during El Niño (La Niña) in the wedge-shaped area, and vice versa in the other area.

Sea-Surface Salinity. The spatial patterns of the interannual mode #1 EOF in SSS (Fig. 2b) roughly isolate part of the western equatorial Pacific with two branches running eastward and south-eastward (<0 values) from, once again, some kind of boomerang-shaped area including the SPCZ (>0 values). The time function presents a very good correspondence with the SOI, the best correlation ($R=-0.88$) being obtained when it lags the SOI by 4 months. Below (above) average SSS appeared during El Niño (La Niña) in regions of negative spatial patterns, and vice versa in the other regions.

0/450 dbar Surface Dynamic Height Anomaly. Fig. 2c shows a near-perfect correlation between the interannual mode #1 EOF time function and the filtered SOI ($R=0.97$ at 1-2 month lag). The prominent feature in the spatial pattern is the presence of positive values in the west and negative values in the east, from about 15°S to 20°N . This means that during the El Niño events the sea level was lower than average in the western half of the basin, whereas it was higher than average in the eastern half; the reverse situation was observed during La Niña events. This results in a zonal “seesaw” structure almost in phase with the SOI, with maximum amplitude located slightly south of the equator and a “fulcrum” near 170°W . The second EOF in surface dynamic height also extracts an ENSO-like signal (not shown here). The time function compares well with the filtered SOI, with a maximum correlation coefficient ($R=-0.53$) obtained when it lags the SOI by as much as 13 months. Interestingly, the time functions of the EOF mode #1 leads the EOF mode #2 by about one year, suggesting a phase propagation. The spatial pattern of the EOF mode #2 approximately separates the 20°S - 5°N from the 5°N - 20°N zonal strips, with maximum amplitudes in the western-central equatorial basin. Longitude-time diagrams (not shown here) indicate that the EOF mode #2 reflects a continuous propagation around the tropical north Pacific, *i.e.*, westward around 14°N , southward along 135°E , eastward around the equator, and then northward along 85°W to close the circuit in 3-4 years. The westward propagation off the equator in the northern hemisphere, as well as the apparent continuity around the tropical North Pacific have been and still are the matter of intense scientific discussions regarding their role on the ENSO cycle (see White *et al.*, 1985; Pazan *et al.*, 1986; Graham and White, 1988, 1991; Battisti, 1989; Kessler, 1990; Zhang and Levitus, 1997).

Surface Wind Stress. The interannual mode #1 EOF in zonal wind is shown in Fig. 2d. The spatial pattern presents large coherent variations spanning almost the entire basin. The spatial pattern in the meridional wind, not shown here, roughly delimits the northern from the southern hemisphere. The zonal wind EOF time function is well correlated with the SOI with maximum correlations obtained when it lags the SOI by two months ($R=0.67$). It signifies that eastward (and equatorward for the meridional component) wind anomalies occurred during the El Niño events, yielding clockwise rotation of the trade winds in the southern hemisphere and counter-clockwise rotation in the northern hemisphere; the reverse anomalies appeared during La Niña events.

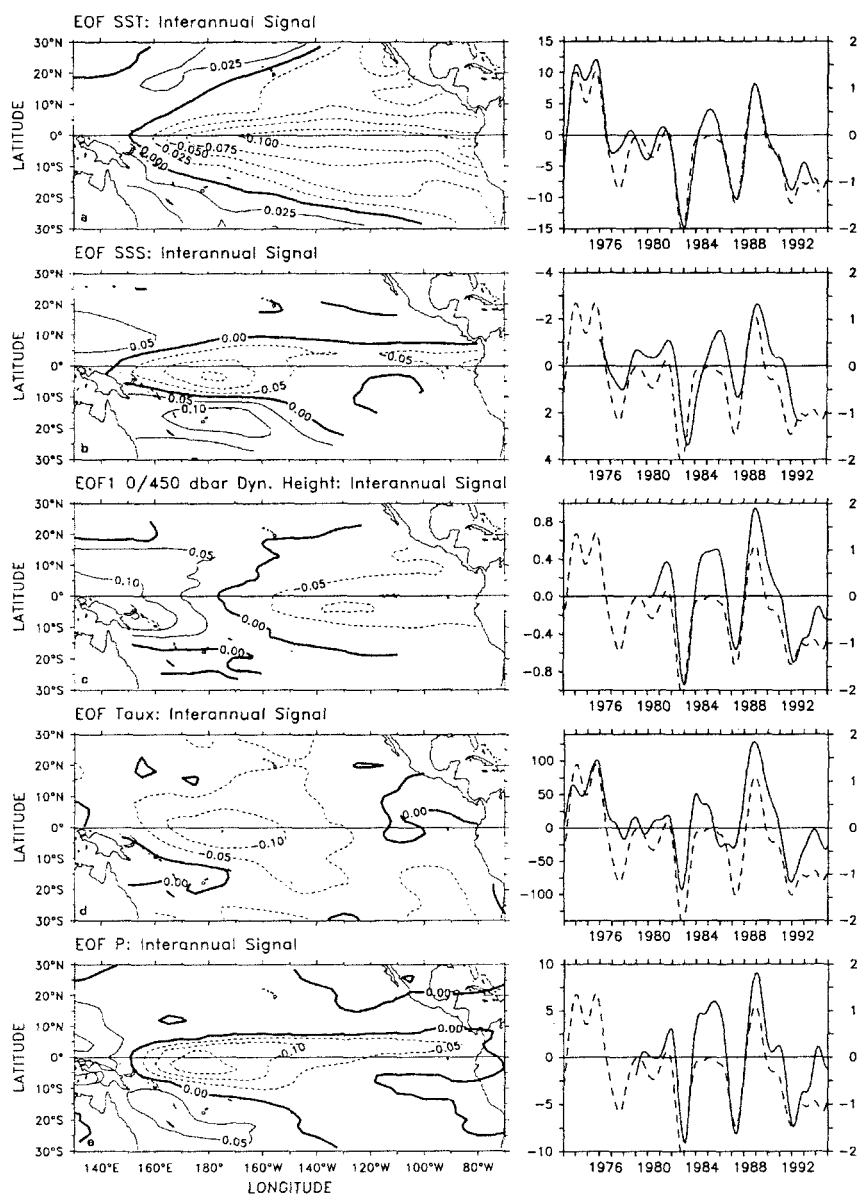


Fig. 2 - Spatial patterns (left panels) and time functions (right panels, full lines, left vertical axes) of the interannual mode #1 EOF in (a) sea-surface temperature, (b) sea-surface salinity, (c) 0/450 dbar dynamic height anomaly, (d) zonal pseudo-stress, and (e) precipitation. On the right panels, note that the scale of the vertical axis increases upward in some cases and downward in others. The dashed lines on the right panels represent the 25-month Hanning filtered Southern Oscillation Index (SOI) scaled on the right vertical axes. The units are defined so that the product between the spatial pattern and the time function denotes (a) Celsius, (c) dyn cm, (d) $\text{m}^2 \text{s}^{-2}$, positive eastward, and (e) m/year.

Precipitation. The time function of the interannual mode #1 EOF for precipitation is well correlated with the filtered SOI ($R=0.9$ at 0-1 month lag) and it captures the major El Niño and La Niña events of 1980-1994 (Fig. 2e). The spatial patterns are generally consistent with numerous studies, back to early in the century, quantifying precipitation changes associated with ENSO (see Ropelewski & Halpert, 1996, and their references). During El Niño, and vice versa during La Niña, we observed below-average P in some kind of boomerang-shaped area stretching from Papua New Guinea towards north and south higher latitudes (> 0 values). Above-average (below-average) P were also observed around the equatorial band during El Niño (La Niña) with extreme anomalies near the dateline (< 0 values).

4. CONCLUSIONS

The present note aimed at presenting a brief overview of the mean structures and of ENSO-related variability in sea-surface temperature (SST), sea-surface salinity (SSS), 0/450 dbar dynamic height anomaly (an alias for sea level), zonal and meridional surface wind stresses, and precipitation (P) in the tropical Pacific. This investigation extends the work of previous publications to encompass the variability of key surface atmospheric and oceanic variables which, in the present case, were all analysed with the same approach, over the whole tropical Pacific, and over a time period long enough to address ENSO variability.

At the ENSO time scale, the amplitude of SST changes was found to be greatest in the central-eastern basin, contrasting: (1) with the SSS, zonal wind and P changes which were found predominant in the western-central basin and (2) with sea level changes which clearly appeared both in the east and in the west. Schematically, in the equatorial band, where the signals are most pronounced, the El Niño (La Niña) events were concerned (1) in the east and centre, with warmer (colder) than average SST and a sea level increase (decrease), and (2) in the west with below (above) average SSS, westerly (easterly) wind anomalies, a rainfall excess (deficit) limited to the east of about 150°E , and a sea level decrease (increase). For perspective, the magnitude of these ENSO changes were equal to or greater than the magnitude of the seasonal changes. Much smaller ENSO changes occurred away from the equatorial band, except in the ITCZ and SPCZ, for SSS, P and meridional wind changes.

Acknowledgements

Some of the data used were provided by scientists from various institutions. It includes P. Arkin J.R. Donguy, M.C. Fabri, C. Hénin, R. Lukas, J. O'Brien, J. Picaut, M. McPhaden, D. Reynolds and P. Xie. I am very thankful for having had the possibility to use all of these data. This work was supported by the "REGIONAL P011" convention between the South Pacific Regional Environment Program (SPREP) and ORSTOM via the *Caisse Française de Développement*, in the framework of the international CLIVAR program (WCRP, 1995).

References cited

- BATTISTI, D. S., 1989 - On the role of off-equatorial oceanic Rossby wave during ENSO. *J. Phys. Oceanogr.*, **19**: 552-559.
- BLACKMAN, R. B. & TUKEY, J. W., 1958 - *The measurement of power spectra*, 190p., New York: Dover publications Inc.
- DELCROIX, T. & HÉNIN, C., 1991 - Seasonal and interannual variations of sea-surface salinity in the tropical Pacific ocean. *J. Geophys. Res.*, **96**: 22135-22150.
- DELCROIX, T., HÉNIN, C., PORTE, V. & ARKIN, P., 1996 - Precipitation and sea-surface salinity in the tropical Pacific Ocean. *Deep Sea Res.*, **43**: 1123-1141.
- DELCROIX, T., 1998 - Observed surface oceanic and atmospheric variability in the Tropical Pacific at seasonal and ENSO time scales: a tentative overview. *J. Geophys. Res.*, **103**: 18611-18633.
- DONGUY, J. R. & HÉNIN, C., 1976 - Relations entre les précipitations et la salinité de surface dans l'océan Pacifique tropical sud-ouest basées sur un échantillonnage de surface de 1956 à 1973. *An. Hydrogr.*, **4**: 53-59.
- GOLDENBERG, S. & O'BRIEN, J. J., 1981 - Time and space variability of tropical wind stress. *Mon. Wea. Rev.*, **109**: 1190-1207.
- GRAHAM, N. E. & WHITE, W. B., 1988 - The El Niño / Southern Oscillation as a natural oscillator of the tropical Pacific ocean-atmosphere system. *Science*, **240**: 1293-1302.
- GRAHAM, N. E. & WHITE, W. B., 1991 - Comments on: On the role of off-equatorial oceanic Rossby waves during ENSO. *J. Phys. Oceanogr.*, **21**: 453-460.
- HÉNIN, C. & GRELET, J., 1996 - A merchant ship thermosalinograph network in the Pacific ocean. *Deep Sea Res.*, **11-12**: 1833-1856.
- KESSLER, W., 1990 - Observations of long Rossby waves in the Northern tropical Pacific. *J. Geophys. Res.*, **95**: 5183-5217.
- LEVITUS, S., 1982 - Climatological atlas of the world ocean. *NOAA Prof. Pap.*, **13**: 173p.; Washington DC: US Govt. Print. Office.
- LEVITUS, S., BURGETT, R. & BOYER, T. P., 1994 - World Ocean Atlas, Volume 3. *in: Salinity. NOAA Atlas, NESDIS, 3*: 97p.; Washington, D.C.: U.S. Dept. of Commerce.
- MCPHADEN, M., FREITAG, P. & SHEPHERD, A., 1990 - Moored salinity time series measurements at 0°, 140°W. *J. Atmos. Ocean. Tech.*, **4**: 568-575.
- MCPHADEN, M., 1993 - TOGA-TAO & The 1991-93 El Niño Southern Oscillation event. *Oceanography*, **6**: 36-44.
- PAZAN, S., WHITE, W., INOUE, M. & O'BRIEN, J., 1986 - Off-equatorial influence upon Pacific equatorial dynamic height variability during the 1982-83 El Niño - Southern Oscillation event. *J. Geophys. Res.*, **91**: 8437-8449.
- PHILANDER, G., 1989 - *El Niño, La Niña, and the southern oscillation*, 293p., San Diego, California: Academic Press.
- RÉBERT, J. P., DONGUY, J. R., ELDIN, G. & WYRTKI, K., 1985 - Relations between sea level, thermocline depth, heat content, and dynamic height in the tropical Pacific. *J. Geophys. Res.*, **90**: 11719-11725.
- REID, J., 1961 - On the geostrophic flow at the surface of the Pacific ocean with respect to the 1000 dbar surface. *Tellus*, **13**: 489-502.
- REYNOLDS, D. & SMITH, T., 1994 - Improved global sea surface temperature analyses using optimum interpolation. *J. Climate*, **7**: 929-948.
- ROPELEWSKI, C. & HALPERT, M., 1996 - Quantifying Southern Oscillation - precipitation relationships. *J. Climate*, **9**: 1043-1059.
- TAYLOR, R. C., 1973 - An atlas of Pacific islands rainfall. *in: Department of Meteorology Publication*, **25**: 165p.; Honolulu, USA: The University of Hawaii, Rep. HIG 73-8, HI 96822.

- WCRP, CLIVAR, 1995 - A study of climate variability and predictability, science plan. *World Climate Research Program publications series*, **89**: 157p.
- WHITE, W., MEYERS, G., DONGUY, J. R., & PAZAN, S., 1985 - Short-term climatic variability in the thermal structure of the Pacific Ocean during 1979-82. *J. Phys. Oceanogr.*, **15**: 917-935.
- WYRTKI, K. & MEYERS, G., 1976 - The trade wind field over the Pacific ocean. *J. App. Met.*, **15**: 698-704.
- XIE, P. & ARKIN, P., 1996 - Analyses of global monthly precipitation using gauge observations, satellite estimates, and numerical model predictions. *J. Climate*, **9**: 840-858.
- ZHANG, R. H. & LEVITUS, S., 1997 - Interannual variability of the coupled tropical Pacific ocean-atmosphere system associated with the El Niño - Southern Oscillation. *J. Climate*, **10**: 1312-1330.

1998

BULLETIN

de l'INSTITUT FRANÇAIS
d'ÉTUDES ANDINES

Tome 27
N° 3



*Variations climatiques et ressources en eau
en Amérique du Sud: Importance et
conséquences des événements
El Niño*



COLOMBIE
ÉQUATEUR
PÉROU
BOLIVIE

IRD

Institut de recherche
pour le développement

CINQUANTENAIRE
1948
1998

IFEA